Biogenesis of lysosome-related organelles complex 3 (BLOC-3): A complex containing the Hermansky–Pudlak syndrome (HPS) proteins HPS1 and HPS4

Ramin Nazarian*, Juan M. Falcón-Pérez*, and Esteban C. Dell'Angelica†

Department of Human Genetics, David Geffen School of Medicine, University of California, Los Angeles, CA 90095

Edited by Pietro V. De Camilli, Yale University School of Medicine, New Haven, CT, and approved June 5, 2003 (received for review April 7, 2003)

Hermansky–Pudlak syndrome (HPS) defines a group of autosomal recessive disorders characterized by deficiencies in lysosome-related organelles such as melanosomes and platelet-dense granules. Several *HPS* genes encode proteins of unknown function including HPS1, HPS3, and HPS4. Here we have identified and characterized endogenous HPS3 and HPS4 proteins from HeLa cells. Both proteins were found in soluble and membrane-associated forms. Sedimentation-velocity and coimmunoprecipitation experiments revealed that HPS4 but not HPS3 associates with HPS1 in a complex, which we term biogenesis of lysosome-related organelles complex 3 (BLOC-3). Mutant fibroblasts deficient in either HPS1 or HPS4 displayed abnormal localization of lysosomes and late endosomes, which were less concentrated at the juxtanuclear region in mutant cells than in control fibroblasts. The coat-color phenotype of young homozygous double-mutant mice deficient in subunits of BLOC-3 (HPS1) and BLOC-1 (pallidin) was indistinguishable from that of BLOC-1 single mutants. Taken together, these observations suggest that HPS1 and HPS4 are components of a protein complex that regulates the intracellular localization of lysosomes and late endosomes and may function in a BLOC-1-dependent pathway for melanosome biogenesis.

Hermansky–Pudlak syndrome (HPS) defines a group of autosomal recessive disorders characterized by oculocutaneous albinism, prolonged bleeding, and mild ceroid lipofuscinosis. A subset of HPS patients also develops granulomatous colitis and pulmonary fibrosis, which is often fatal (1). Abnormal pigmentation and bleeding are associated with defects in the biogenesis of two specialized lysosome-related organelles: melanosomes (2) and platelet-dense granules (3). The cellular bases for the other clinical manifestations are poorly understood, although they may also arise from defects in organelles of the lysosomal system.

HPS-causing mutations have been identified in several human genes (1). One of these genes encodes the β3A subunit of AP-3, a protein complex that mediates signal-dependent trafficking of integral membrane proteins to lysosomes and related organelles (4). The products of other identified *HPS* genes including HPS1, HPS3, and HPS4 display no homology to any known protein and seem not to be required for AP-3-dependent trafficking (5). Initial characterization of the HPS1 protein revealed that it is expressed ubiquitously, can exist as cytosolic and membrane-associated species, and may be part of a complex (6, 7). Neither HPS3 nor HPS4 have been characterized biochemically.

Here we report identification of endogenous HPS3 and HPS4 from human HeLa cells. We show that both proteins exist in soluble and membrane-bound forms and that HPS4 is associated with HPS1 in a stable complex, named biogenesis of lysosome-related organelles complex 3 (BLOC-3). We provide evidence for a role of BLOC-3 in regulating the localization of lysosomes and late endosomes in fibroblasts and for its possible functional relationship to BLOC-1, another protein complex implicated in the biogenesis of lysosome-related organelles (8, 9).

Materials and Methods

DNA Constructs. The following plasmids were generated by PCR-based engineering of cDNA segments encoding the indicated fragments of human proteins and cloning in-frame into the *Eco*RI–*Sal*I sites of pGEX-5X-1 (pGST, Amersham Pharmacia Biotech), pET-30a(+) (pHIS, Novagen), pET-43.1a(+) (pNUS, Novagen), pGBT9, or pGAD424 (Becton Dickinson Biosciences): pGST-HPS3c and pNUS-HPS3c (residues 820-1004 of HPS3); pGST-HPS4b (residues 187–384 of HPS4); pGST-HPS4c and pHIS-HPS4c (residues 385–534 of HPS4); pGBT9-HPS1 and pGAD424-HPS1 (full-length HPS1); and pGBT9-HPS4 and pGAD424-HPS4 (full-length HPS4). For phenotype-rescue experiments, the complete ORFs of human HPS1 and HPS4 were cloned into pCR3.1 (Invitrogen). All constructs were verified by DNA sequencing.

Purification of Recombinant Proteins. His_6-tagged and GST fusion proteins were expressed in *Escherichia coli* and affinity-purified as described (8). The fusion protein NusA-HPS3c, encoded by plasmid pNUS-HPS3c, was expressed in *E. coli* BL21-CodonPlus-(DE3)-RP (Stratagene) and affinity-purified by using S-Protein agarose (Novagen) according to manufacturer instructions.

Antibodies. The HP3c, HP4b, and HP4c polyclonal antibodies were obtained by immunizing rabbits with purified GST-HPS3c, GST-HPS4b, and GST-HPS4c fusion proteins, respectively. The antibodies were purified by affinity chromatography with specific ligands covalently bound to Affi-Gel 15 beads (Bio-Rad), as follows: HP3c was purified by using NusA-HPS3c; HP4b was purified by using GST-HPS4b and subsequently adsorbed by using GST; and HP4c was purified by using His_6-HPS4c. The anti-HPS1 rabbit polyclonal antibody was raised against a synthetic peptide comprising residues 253–267 of human HPS1 and affinity-purified by using the peptide as a ligand (6). The mAb 6C4 against lysobisphosphatidic acid (LBPA) was kindly provided by J. Gruenberg (University of Geneva, Geneva). Rat mAb 1D4B to mouse lysosome-associated membrane protein 1 (Lamp-1) and mouse mAbs to human Lamp-1 (H4A3) and Lamp-2 (H4B4) were purchased from the Development Studies Hybridoma Bank (Iowa City, IA). Mouse mAb to early endosome antigen 1 (EEA1) was from Becton Dickinson Biosciences. Mouse mAb H68.4 to transferrin receptor was from Zymed. Cy3-conjugated secondary antibodies were from Jackson Immu-

This paper was submitted directly (Track II) to the PNAS office.

Abbreviations: HPS, Hermansky–Pudlak syndrome; BLOC, biogenesis of lysosome-related organelles complex; LBPA, lysobisphosphatidic acid; Lamp, lysosome-associated membrane protein; EEA1, early endosome antigen 1.

*R.N. and J.M.F.-P. contributed equally to this work.

†To whom correspondence should be addressed at: Department of Human Genetics, University of California, Gonda 6357B, Los Angeles, CA 90095-7088. E-mail: edellangelica@mednet.ucla.edu.

www.pnas.org/cgi/doi/10.1073/pnas.1532040100

noResearch. Alexa 488-conjugated secondary antibodies were from Molecular Probes.

Mouse Strains. The mouse strains light ear (C57BL/6J-*Hps4*$^{le/le}$), pale ear (C57BL/6J-*Hps1*$^{ep/ep}$), and pallid (C57BL/6J-*Pldn*$^{pa/pa}$) were kindly provided by Juan S. Bonifacino (National Institutes of Health) and Richard T. Swank (Roswell Park Cancer Institute, Buffalo, NY). C57BL/6J mice were used as wild-type controls. Pallid/pale-ear double mutants were generated by crossing homozygous pale-ear and pallid mice followed by crossing of the F_1 double-heterozygous mice. The genotypes of selected F_2 mice were determined by RT-PCR followed by agarose gel electrophoresis (for *Hps1* alleles) or sequencing (for *Pldn* alleles).

Cell Culture. Skin fibroblast cultures from wild-type and mutant mice were obtained by incubating minced dermis with complete DMEM/20% FBS [DMEM supplemented with 20% (vol/vol) FBS, 2 mM glutamine, 0.1 g/liter streptomycin, and 100 units/ml penicillin] in plastic dishes at 37°C in a tissue-culture incubator. Primary skin fibroblast cultures derived from an HPS patient homozygous for a 16-bp duplication in exon 15 of *HPS1* (GM14609) and an apparently normal individual (GM00316A) were obtained from Coriell Cell Repositories (Camden, NJ) and maintained in complete DMEM/20% FBS. Human HeLa cells were purchased from the American Type Culture Collection and grown in complete DMEM/10% FBS.

Biochemical Procedures. HeLa cells were metabolically labeled with [^{35}S]Met and [^{35}S]Cys for 18–22 h. For subcellular fractionation studies, labeled cells were washed with ice-cold PBS, suspended in homogenization buffer [50 mM Hepes (pH 7.4)/1 mM EGTA/1 mM DTT/0.5 mM $MgCl_2$/0.1% (wt/vol) BSA/1 mM 4-(2-aminoethyl)-benezesulfonyl fluoride/10 mg/liter leupeptin/5 mg/liter aprotinin/1 mg/liter pepstatin A], and lysed by successive passages through a 25-gauge needle. The crude extract was centrifuged at 13,000 $\times$ *g* for 10 min at 4°C and then at 120,000 $\times$ *g* for 90 min at 4°C to obtain cytosolic and microsomal membrane fractions. Microsomal membranes were washed once in homogenization buffer to reduce contamination by cytosolic proteins. Sedimentation-velocity analyses were performed as described (8) except that samples were centrifuged for 20 h and the resulting fractions were analyzed by immunoprecipitation recapture. Immunoprecipitation recapture was carried out as described (10) except that the first immunoprecipitation step included an additional wash with 0.01% (wt/vol) SDS. Yeast two-hybrid assays were performed as described (8).

Fluorescence Microscopic Analyses. Fibroblasts were grown on glass coverslips by using complete DMEM/20% FBS medium. For phenotype-rescue experiments, cells were transfected ≈24 h before analysis with expression plasmids encoding HPS1 or HPS4 by using the FuGENE 6 transfection reagent (Roche Molecular Biochemicals). For labeling of lysosomes with dextran, cells were incubated for 16 h at 37°C in medium containing 5 g/liter Texas red-conjugated fixable dextran (Molecular Probes) followed by a 4-h chase period in medium lacking dextran. Lysosome labeling with LysoTracker red DND-99 (Molecular Probes) was carried out per manufacturer instructions. In some experiments, cells were incubated for 90 min at 37°C in medium containing 30 μM nocodazole followed by a recovery period of up to 90 min in medium lacking the drug. Indirect immunofluorescence was performed as described (10) except for staining with mAb 6C4, which was carried out by using an alternative protocol (11). Stained cells were examined by using a Zeiss Axioskop 2 microscope or, for colocalization analyses, a Leica TCS SP multiphoton confocal microscope. For the analyses reported in Table 1, cells were scored under the microscope for perinuclear or dispersed distribution of each marker by using a "blind test" in which the examiner was not aware of the identity of the cell line present in each coverslip. For each marker, experimental condition, and cell line, an average of 406 cells was scored. For phenotype-rescue experiments, an average of 74 transfected cells was scored by using the same blinded approach.

Table 1. Perinuclear accumulation of markers of late endosomes and lysosomes in fibroblasts from wild-type and BLOC-3-deficient mice

Marker	Treatment	Wild type	Pale ear (*Hps1*$^{ep/ep}$)	Light ear (*Hps4*$^{le/le}$)
Lamp-1	None	50 ± 10	13 ± 2*	26 ± 5*
	+HPS1 plasmid	66 ± 11	52 ± 3†	—‡
	+HPS4 plasmid	60 ± 6	—‡	66 ± 11†
	Nocodazole/recovery§	48 ± 12	7 ± 3*	18 ± 2*
Dextran¶	None	62 ± 6	28 ± 10*	36 ± 1*
	Nocodazole/recovery§	56 ± 2	16 ± 6*	23 ± 7*
LBPA‖	None	50 ± 16	14 ± 8*	—‡

Values represent percentages of cells displaying pronounced perinuclear accumulation and are expressed as means ± SD of two to three independent cell lines.
*Student's *t* test: $P < 0.05$ versus wild-type cells.
†Student's *t* test: $P < 0.01$ versus nontransfected cells.
‡Not determined.
§Prior to fixation, cells were incubated in medium containing 30 μM nocodazole for 90 min and then in nocodazole-free medium for another 90 min.
¶Internalization of Texas red-conjugated dextran was performed for 16 h followed by a 4-h chase period.
‖mAb 6C4 immunoreactivity.

Results

Biochemical Characterization of HPS3 and HPS4 Proteins. We raised three affinity-purified rabbit polyclonal antibodies, one of them (HP3c) against the last 185 residues of human HPS3 and the others (HP4b and HP4c) against two distinct internal regions of human HPS4. The antibodies specifically recognized recombinant forms of HPS3 or HPS4, although they failed to detect the endogenous proteins from various cell types by immunoblotting or immunofluorescence (data not shown). This is probably due to low antibody sensitivity and/or low relative abundance of the antigen. Nevertheless, the antibodies allowed for unambiguous detection of endogenous HPS3 and HPS4 in HeLa cells by immunoprecipitation recapture, in which the antigen was immunoprecipitated first under native conditions, denatured, and "recaptured" in a second immunoprecipitation step. Human HPS4 was isolated as a single radiolabeled protein that migrated on SDS/PAGE gels as an ≈100-kDa polypeptide (Fig. 1*A*). The protein was isolated by using either HP4b or HP4c antibodies for both immunoprecipitation steps (Fig. 1*A*, lanes 2 and 5) or one antibody for the first immunoprecipitation and the other for the recapture step (Fig. 1*A*, lanes 8 and 10). As expected, the protein was not detected in control experiments in which irrelevant IgG was used at either step (Fig. 1*A*). Similar experiments with the HP3c antibody resulted in isolation of HPS3 as a single radiolabeled protein of an apparent molecular mass of ≈130 kDa, which was not detected in control immunoprecipitations by using irrelevant IgG at either step (Fig. 1*B*).

The deduced amino acid sequences of HPS3 and HPS4 predict no transmembrane domains or specific targeting motifs. To determine whether HPS3 and HPS4 were cytosolic proteins, metabolically labeled HeLa cells were lysed in the absence of detergents, and the soluble and postnuclear membrane fractions were isolated by differential centrifugation. The two proteins were consistently recovered from both fractions (Fig. 1*C*). In addition, the membrane-associated forms of HPS3 and HPS4

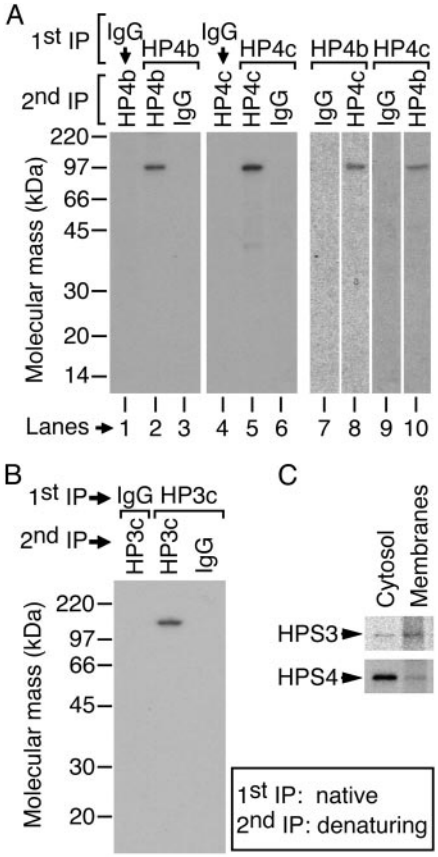

Fig. 1. (*A* and *B*) Identification of endogenous HPS4 (*A*) and HPS3 (*B*) proteins from HeLa cells by immunoprecipitation recapture. Cells metabolically labeled with [^{35}S]Met and [^{35}S]Cys were lysed in the presence of 1% (wt/vol) Triton X-100 and immunoprecipitated with control rabbit IgG, rabbit antibody HP3c to HPS3, or rabbit antibodies HP4b and HP4c to HPS4. After extensive washing, each first immunoprecipitate (1st IP) was denatured by heating in the presence of SDS and DTT, diluted, and immunoprecipitated again (2nd IP) by using the indicated antibodies. Washed immunoprecipitates were analyzed by 4–20% SDS/PAGE followed by fluorography. (*C*) Cytosolic and microsomal membrane fractions from metabolically labeled HeLa cells were prepared by differential centrifugation and subjected to immunoprecipitation recapture by using HP3c antibody to HPS3 and HP4c antibody to HPS4.

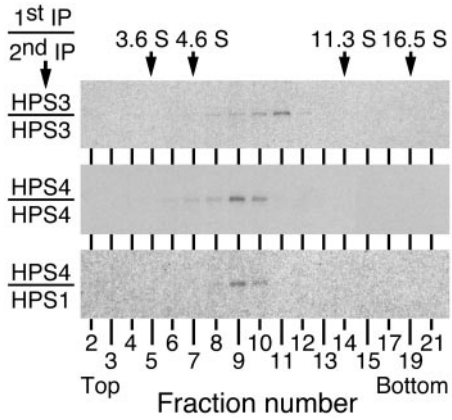

Fig. 2. Sedimentation-velocity analysis of HPS proteins. Cytosol from metabolically labeled HeLa cells was fractionated by centrifugation on a linear 5–20% (wt/vol) sucrose gradient. Each fraction was subjected to immunoprecipitation recapture by using antibody HP3c to detect HPS3, antibody HP4c to detect HPS4, or a combination of HP4c antibody in the first immunoprecipitation (1st IP) and anti-HPS1 in the second immunoprecipitation (2nd IP) to detect HPS1 protein associated to HPS4. Not shown are fractions 1, 16, 18, and 20, which contained none of these proteins. The positions in the gradient of standard proteins of known sedimentation coefficient (in Svedberg units) are indicated at the top.

could be quantitatively extracted with sodium carbonate, pH 11 (data not shown). Thus, HPS3 and HPS4 can behave as both soluble and peripheral membrane proteins.

Next we examined the sedimentation properties of the soluble forms of HPS3 and HPS4 under native conditions by ultracentrifugation of HeLa cytosol on a sucrose gradient followed by immunoprecipitation-recapture analysis of each fraction. As shown in Fig. 2, the rate of sedimentation of HPS3 was higher than that of HPS4, suggesting that these two proteins may not associate with each other into a stable complex. By comparing the positions in the gradient of HPS3 and HPS4 to those of standard proteins, the sedimentation coefficients were estimated to be 8.8 ± 1.0 S for HPS3 and 6.9 ± 0.9 S for HPS4.

HPS4 but Not HPS3 Is a Subunit of a Stable Complex Containing HPS1. It has been speculated that HPS1 and HPS4 interact with each other (12, 13). To test for stable physical association between HPS1 and HPS4, we performed coimmunoprecipitation experiments by using the immunoprecipitation-recapture procedure described above. As expected, both HPS1 and HPS4 were recovered from samples in which their corresponding antibodies were used for both steps (Fig. 3, lanes 1, 5, and 10). Importantly, HPS1 was also recovered from samples first immunoprecipitated by using antibodies to HPS4 (Fig. 3, lanes 3 and 7), and conversely, HPS4 was recovered from a sample first immunoprecipitated by using anti-HPS1 (Fig. 3, lane 12). Neither HPS1 nor HPS4 were found in samples first immunoprecipitated by using an antibody to HPS3 (Fig. 3, lanes 16–18), and HPS3 was not detected in samples first immunoprecipitated by using antibodies to HPS1 or HPS4 (Fig. 3, lanes 4, 8, and 13). We observed association of HPS1 with both soluble and membrane-bound forms of HPS4 (data not shown) and found HPS1 associated with the bulk of cytosolic HPS4 upon fractionation on a sucrose gradient (Fig. 2 *Bottom*). Taken together, these results indicate that endogenous HPS1 and HPS4 are components of a stable protein complex. We have named this complex BLOC-3.

Abnormal Distribution of Lysosomes and Late Endosomes in Cells Deficient in BLOC-3 Subunits. To gain insights into the possible function of BLOC-3 in cells that contain conventional lysosomes but lack lysosome-related organelles, we derived immortalized cell lines of skin fibroblasts from homozygous mutant mice deficient in HPS1 (pale ear) and HPS4 (light ear) as well as from isogenic "wild-type" control mice. By immunofluorescence analyses of fixed, permeabilized cells, we noticed that the distribution of Lamp-1, an endogenous membrane protein marker of late endosomes and lysosomes, was relatively less concentrated in the perinuclear region of pale-ear and light-ear fibroblasts than in the same region of control cells (Fig. 4 *A* and *B* and data not shown). To explore this issue further, we determined percentages of cells displaying perinuclear accumulation of Lamp-1 by examination under the fluorescence microscope of at least two independent cell lines derived from each mouse strain. As an attempt to overcome the intrinsic subjectivity of this analysis, we used a blind test strategy in which the examiner was not aware of the identity of the samples. The results are listed in Table 1. Approximately half of the immortalized fibroblasts derived from our wild-type mouse skin preparations displayed a strong perinuclear accumulation of Lamp-1-positive organelles, in many cases with few Lamp-1-positive structures at the cell periphery (Fig. 4*A*, arrows, and Table 1). In contrast, the frequency of cells displaying this phenotype was reduced for pale-ear and, to a

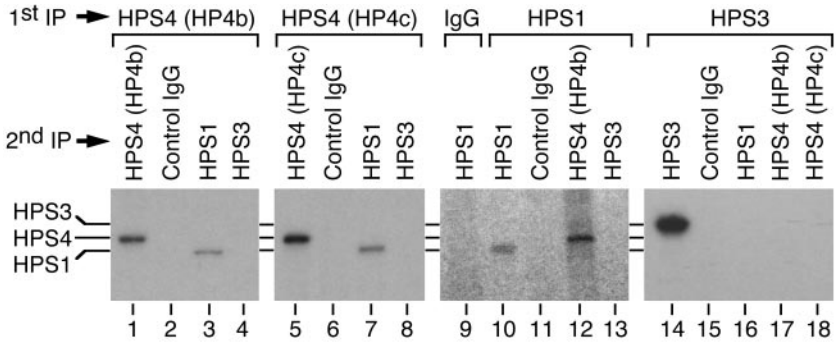

Fig. 3. Coimmunoprecipitation of HPS1 and HPS4. HeLa cells metabolically labeled with [^{35}S]Met and [^{35}S]Cys were lysed under nondenaturing conditions. The cleared lysate was subjected to a first immunoprecipitation (1st IP) by using control rabbit IgG or purified rabbit antibodies to HPS4 (either HP4b or HP4c antibodies), HPS1, or HPS3. After extensive washing, the immunoprecipitates were treated by heating in the presence of SDS and DTT, diluted, and subjected to a second immunoprecipitation (2nd IP) by using the indicated antibodies. Final immunoprecipitates were analyzed by SDS/PAGE and fluorography.

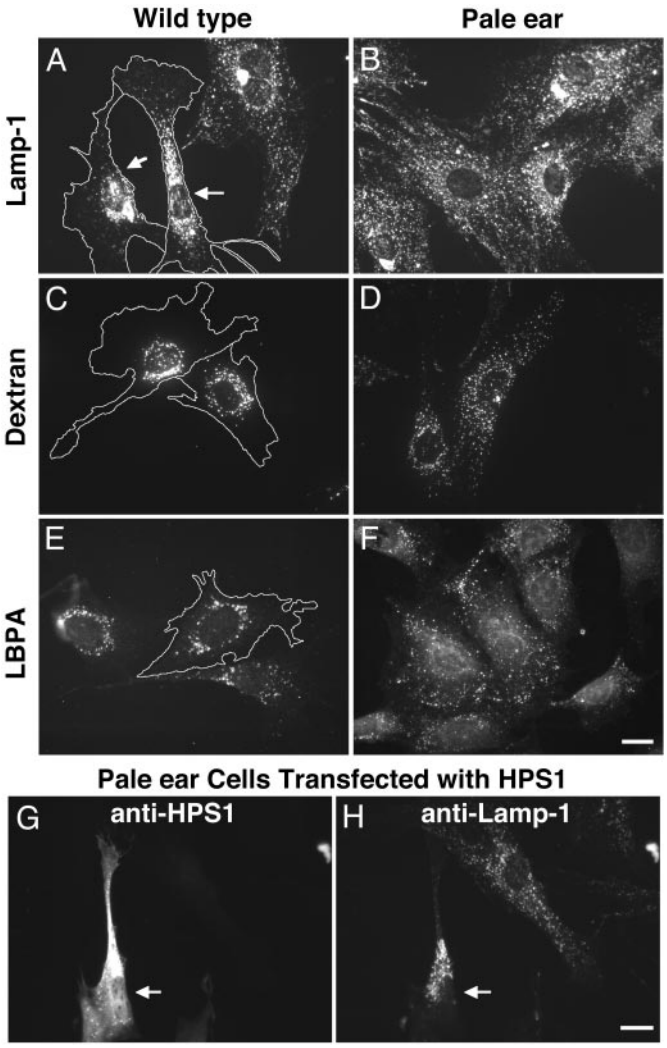

Fig. 4. Intracellular distribution of markers of late endosomes and lysosomes in fibroblasts from wild-type and mutant mice. Skin fibroblasts from wild-type C57BL-6J (*A*, *C*, and *E*) and HPS1-deficient pale-ear (*B*, *D*, and *F–H*) mice were grown on glass coverslips. Cells were stained by using mAb 1D4B to Lamp-1 (*A* and *B*) or mAb 6C4 to LBPA (*E* and *F*), loaded with Texas red-conjugated dextran (*C* and *D*) or transiently transfected with plasmid encoding human HPS1 and subsequently stained with rabbit antibodies to HPS1 (*G*) together with mAb 1D4B to Lamp-1 (*H*). The perimeters of selected cells are highlighted by white lines that were drawn based on an overexposed version of the same image. (Bars, 20 μm.)

lesser extent, light-ear fibroblasts (Table 1). Immunoblotting analyses (not shown) indicated that all these cell lines expressed similar levels of Lamp-1 protein, suggesting that the observed differences were not secondary to abnormal Lamp-1 biosynthesis or degradation. We also examined a primary skin fibroblast culture from a patient suffering from HPS1 disease and observed a reduced percentage of cells displaying perinuclear accumulation of endogenous Lamp-2 as compared with that of fibroblasts from a normal individual (26% and 76%, respectively; Lamp-1 distribution was not analyzed because of differences in protein expression levels; data not shown). Importantly, the Lamp-1 distribution defects observed in pale-ear and light-ear cells could be restored by transient expression of HPS1 and HPS4 proteins, respectively (Fig. 4 *G* and *H* and Table 1), indicating that abnormal Lamp-1 localization indeed was a consequence of BLOC-3 deficiency.

Next we performed a series of experiments to test whether the abnormal Lamp-1 distribution observed in BLOC-3-deficient fibroblasts was due to defects in Lamp-1 trafficking to late endosomes and lysosomes or, alternatively, to impaired movement/localization of these organelles.

First we tested whether Lamp-1 localization to lysosomes was compromised in mutant cells. We labeled lysosomes of wild-type and pale-ear cells with fluorescent dextran and determined degrees of colocalization with endogenous Lamp-1 by confocal microscopy. Because transport of fluid-phase markers to lysosomes could be delayed, in principle, in pale-ear cells, we loaded cells with dextran for 16 h followed by a long (4-h) chase period to ensure specific lysosome labeling. No differences were observed between wild-type and mutant cells in the relative numbers of dextran-labeled structures that were also positive for Lamp-1 or of Lamp-1-positive structures that contained no detectable dextran (Table 2). We also observed extensive colocalization of Lamp-1 with lysosomes labeled with a low-pH

Table 2. Estimation of degrees of colocalization between Lamp-1 and lysosomes labeled with internalized dextran or EEA1-positive early endosomes in wild-type and pale-ear fibroblasts

Calculated parameter	Wild type	Pale ear (*Hps1*$^{ep/ep}$)
Lamp-1$^+$ Dextran$^+$/Dextran$^+$	82 ± 7	81 ± 6
Lamp-1$^+$ Dextran$^-$/Lamp-1$^+$	39 ± 3	36 ± 3
Lamp-1$^+$ EEA1$^+$/Lamp-1$^+$	16 ± 2	14 ± 1

Values are expressed as means ± SD (n = 2) and represent percentages of the structures conforming to the definitions indicated in numerators out of the total number of structures scored positive for the marker indicated in the denominators. Total numbers of scored structures per sample ranged from 307 to 1,049. See *Materials and Methods* for experimental details.

indicator, LysoTracker, both in wild-type and mutant cells (data not shown). In addition, we tested whether the degree of colocalization of Lamp-1 with a marker of early endosomes, EEA1, was increased in mutant cells. However, no difference was found between wild-type and pale-ear fibroblasts in the percentage of Lamp-1-positive structures that were also positive for EEA1 (Table 2). These results argue against the possibility that the peripheral Lamp-1 distribution observed in BLOC-3-deficient cells is a consequence of gross mistargeting of Lamp-1 to peripheral organelles such as early endosomes.

Second, we examined the intracellular distribution of several markers of the endosomal/lysosomal system. We observed in mutant cells reduced perinuclear accumulation of lysosomes labeled with dextran (Fig. 4 *C* and *D* and Table 1) and LysoTracker (data not shown) as well as late endosomes containing the endogenous lipid marker LBPA (Fig. 4 *E* and *F* and Table 1). In contrast, we did not detect any defect in the distributions of markers of early and/or recycling endosomes, namely EEA1 and the transferrin receptor (data not shown). These results demonstrate that localization of late endosomes and lysosomes, not just of the Lamp proteins, is affected in BLOC-3-deficient cells.

Third, we tested the effects of reversible dispersion of lysosomes by a microtubule depolymerization agent, nocodazole, in wild-type and mutant cells. After incubation in the presence of nocodazole for 90 min, the distributions of Lamp-1-positive structures in wild-type and mutant cells were widely peripheral and virtually indistinguishable (data not shown). Within 90 min after nocodazole treatment, wild-type fibroblasts recovered their steady-state Lamp-1 distribution almost completely (Table 1). However, mutant cells seemed to be relatively less efficient in recovering from nocodazole treatment (Table 1). Similar results were obtained by using internalized dextran as a marker of lysosomes (Table 1).

Taken together, these observations are consistent with a role for BLOC-3 in regulating localization of lysosomes and late endosomes to the perinuclear area of the cell.

Coat-Color Phenotype of Mice Deficient in Both BLOC-1 and BLOC-3. To test for a possible functional relationship between BLOC-1 and BLOC-3 in melanosome biogenesis, we generated a homozygous double-mutant mouse strain carrying the null recessive mutations pallid (which affects the pallidin subunit of BLOC-1) and pale ear. F_2 mice resulting from the crossing of pallid/pale-ear double heterozygotes displayed the coat-color phenotypes characteristic of wild-type, pale-ear, or pallid mice, but none of them exhibited a new coat color (Fig. 5). Subsequent genotype analysis indicated that a subset of the F_2 mice displaying pallid-like color phenotype actually were homozygous for both pallid and pale-ear mutations (Fig. 5). Hence, HPS1/BLOC-3 deficiency did not enhance or reduce the pigmentation defect caused by pallidin/BLOC-1 deficiency.

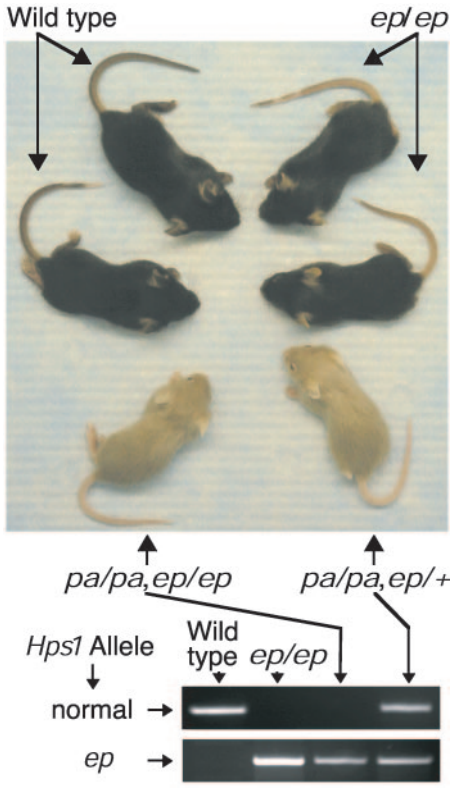

Fig. 5. (*Upper*) Coat-color phenotype of 2-week-old mice carrying the pale-ear and/or pallid mutations as compared with control wild-type mice of the same age. Homozygous pale-ear mice (*ep*/*ep*) display a characteristic reduction in pigmentation in the tail and ears, whereas homozygous pallid mice (*pa*/*pa*) display a generalized pigment dilution. (*Lower*) Result of RT-PCR analysis to verify the presence of wild-type (normal) and mutant (*ep*) *Hps1* alleles in two mice known to be homozygous for the pallid mutation (as inferred by DNA sequencing).

Discussion

Although HPS defects are manifested mainly in cell-type-specific organelles, all known *HPS* genes are expressed ubiquitously (1). In this work we identified HPS3 and HPS4 proteins in HeLa cells, which contain conventional lysosomes but lack specialized lysosome-related organelles. Both proteins displayed mobilities on SDS/PAGE gels that were somewhat lower than expected from their predicted molecular masses (i.e., ≈114 and ≈77 kDa for HPS3 and HPS4, respectively). It remains to be determined whether these abnormal electrophoretic mobilities are due to intrinsic properties of the polypeptide chains or posttranslational modifications. Similar to all HPS proteins characterized thus far, HPS3 and HPS4 were found in both soluble (cytosolic) and membrane-associated pools.

Density gradient fractionation and coimmunoprecipitation experiments suggest that HPS3 and HPS4 are unlikely to associate with each other into a stable complex. Instead, our results revealed that HPS4 is a component of a previously uncharacterized complex, BLOC-3, which also contains HPS1. Interaction was demonstrated by coimmunoprecipitation of endogenous proteins in either soluble or membrane-associated forms and by comigration on a sucrose gradient. On the other hand, we have been unable to demonstrate direct interaction between HPS1 and HPS4 by using the yeast two-hybrid system, and immunodepletion of HPS4 failed to completely deplete HPS1 from labeled HeLa extracts (data not shown). Although technical reasons could explain them, these negative results still raise the possibilities that HPS1 and HPS4 might not be the only subunits of BLOC-3 and that HPS1 species not associated with HPS4 might exist. Nevertheless, the finding that HPS1 and HPS4 are part of a stable complex provides a molecular explanation for the close similarity in phenotypes of pale-ear, light-ear, and pale-ear/light-ear double-mutant mice (12) and for the apparent lack of detectable HPS1 protein found in HPS4-deficient platelets from light-ear mice (13). In addition, it suggests that HPS disease caused by mutations in *HPS4* should be clinically similar to that caused by mutations in *HPS1*, which has been studied extensively and linked to a high risk of developing fatal pulmonary fibrosis (1, 14).

Results described herein provide some insight into the function of BLOC-3 in cells that lack lysosome-related organelles. We found that the intracellular distribution of lysosomes and late

endosomes is affected in fibroblasts deficient in HPS1 or HPS4. Thus, organelles containing markers of lysosomes (dextran or LysoTracker), late endosomes (LBPA), or both (Lamps) were consistently less concentrated at the perinuclear region of mutant cells as compared with distributions of these organelles in control fibroblasts. These effects seemed to be more pronounced in pale-ear fibroblasts than in light-ear cells; although the basis for this difference remains unknown, it could imply the existence of some residual activity in light-ear fibroblasts. Importantly, abnormal Lamp-1 distribution could be rescued in pale-ear and light-ear cells by expression of human HPS1 and HPS4, respectively. Other organelles of the endosomal system, i.e., early and recycling endosomes, were not noticeably affected in BLOC-3-deficient cells, nor was the trans-Golgi network as labeled with antibodies to TGN46 (data not shown). Colocalization experiments with confocal microscopy failed to detect gross mistargeting of Lamp-1 in mutant cells, arguing against the possibility that abnormal Lamp distribution could be a consequence of defective protein trafficking. Rather, our results are more consistent with the idea that movement of lysosomes and late endosomes is defective in BLOC-3-deficient cells. Along these lines, it is noteworthy that phenotypic differences between wild-type and mutant cells were somewhat enhanced by reversible dispersion of lysosomes after treatment with nocodazole (Table 1). These considerations lead us to propose that BLOC-3 is required for optimal movement of these organelles toward the perinuclear region of the cell. Time-lapsed microscopy experiments with cells labeled with fluorescent lysosome markers should allow us to test this idea more directly.

Previous studies have established that movement of lysosomes in mammalian cells depends on both microtubules and the actin cytoskeleton, with the former mediating long-range transport toward both the perinuclear area and the periphery of the cell and the latter mediating short-range movements (ref. 15 and references therein). Proteins reported to regulate movement of late endosomes and lysosomes toward the perinuclear area include Rab7 (a small GTPase of the Rab protein family) (16) and its effector, Rab-interacting lysosomal protein (RILP) (17, 18). RILP was reported recently to induce recruitment of dynactin, an activator of the minus-end-directed motor dynein, to late endosomes and lysosomes (18). Interference with the function of any of these proteins results in dispersion of lysosomes throughout the cell periphery (16–20), which is reminiscent of the phenotype reported herein for BLOC-3-deficient fibroblasts.

Published evidence suggests that the function of the AP-3 complex in the biogenesis of lysosome-related organelles, including melanosomes, is independent of BLOC-1 and BLOC-3 despite the association of these three complexes with HPS disease in humans or mice (refs. 8 and 21 and references therein). To test for a possible functional link between BLOC-1 and BLOC-3, we generated a double-mutant mouse strain homozygous for the pallid and pale-ear mutations. Similar genetic analyses in mice have established that each of the pallid and pale-ear mutations can yield enhanced pigment dilution phenotypes when combined with mutations in other components of the machinery involved in melanosome biogenesis. Thus, the pale-ear mutation, which on its own generates a mild coat-color phenotype, significantly enhanced the pigmentation defects caused by the pearl and beige mutations affecting the β3A subunit of AP-3 and the Chediak–Higashi syndrome 1 protein, respectively (21, 22). Likewise, the pigmentation defect of homozygous pallid/beige double mutants was found to be more severe than that of pallid or beige single mutants (E. K. Novak and R. T. Swank, personal communication). Our results indicate that the color phenotype of pallid/pale-ear double mutants is virtually indistinguishable from that of pallid single mutants, implying that pale ear does not enhance or complement the pigmentation defect caused by the pallid mutation. This apparent absence of genetic interaction is consistent with the notion that BLOC-1 and BLOC-3 may function in the same pathway for melanosome biogenesis.

Note Added in Proof. The association of HPS1 and HPS4 into a complex was reported independently by two recent papers (23, 24).

We thank J. Gruenberg, J. S. Bonifacino, and R. T. Swank for their generous gifts of reagents; D. E. Krantz, C. A. Ghiani, G. S. Payne, and the members of the Dell'Angelica Laboratory for critical reading of the manuscript; and the reviewers for helpful suggestions. This work was supported by National Institutes of Health Grant HL68117.

1. Huizing, M., Boissy, R. E. & Gahl, W. A. (2002) *Pigm. Cell. Res.* **15,** 405–419.
2. Marks, M. S. & Seabra, M. C. (2001) *Nat. Rev. Mol. Cell Biol.* **2,** 738–748.
3. King, S. M. & Reed, G. L. (2002) *Semin. Cell Dev. Biol.* **13,** 293–302.
4. Robinson, M. S. & Bonifacino, J. S. (2001) *Curr. Opin. Cell Biol.* **13,** 444–453.
5. Starcevic, M., Nazarian, R. & Dell'Angelica, E. C. (2002) *Semin. Cell Dev. Biol.* **13,** 271–278.
6. Dell'Angelica, E. C., Aguilar, R. C., Wolins, N., Hazelwood, S., Gahl, W. A. & Bonifacino, J. S. (2000) *J. Biol. Chem.* **275,** 1300–1306.
7. Oh, J., Liu, Z.-X., Feng, G. H., Raposo, G. & Spritz, R. A. (2000) *Hum. Mol. Genet.* **9,** 375–385.
8. Falcón-Pérez, J. M., Starcevic, M., Gautam, R. & Dell'Angelica, E. C. (2002) *J. Biol. Chem.* **277,** 28191–28199.
9. Moriyama, K. & Bonifacino, J. S. (2002) *Traffic* **3,** 666–677.
10. Dell'Angelica, E. C., Ohno, H., Ooi, C. E., Rabinovich, E., Roche, K. W. & Bonifacino, J. S. (1997) *EMBO J.* **16,** 917–928.
11. Incardona, J. P., Gruenberg, J. & Roelink, H. (2002) *Curr. Biol.* **12,** 983–995.
12. Meisler, M. H., Wanner, L. & Strahler, J. (1984) *J. Hered.* **75,** 103–106.
13. Suzuki, T., Li, W., Zhang, Q., Karim, A., Novak, E. K., Sviderskaya, E. V., Hill, S. P., Bennett, D. C., Levin, A. V., Nieuwenhuis, H. K., *et al.* (2002) *Nat. Genet.* **30,** 321–324.
14. Brantly, M., Avila, N. A., Shotelersuk, V., Lucero, C., Huizing, M. & Gahl, W. A. (2000) *Chest* **117,** 129–136.
15. Cordonnier, M.-N., Dauzonne, D., Louvard, D. & Coudrier, E. (2001) *Mol. Biol. Cell* **12,** 4013–4029.
16. Bucci, C., Thomsen, P., Nicoziani, P., McCarthy, J. & van Deurs, B. (2000) *Mol. Biol. Cell* **11,** 467–480.
17. Cantalupo, G., Alifano, P., Roberti, V., Bruni, C. B. & Bucci, C. (2001) *EMBO J.* **20,** 683–693.
18. Jordens, I., Fernandez-Borja, M., Marsman, M., Dusseljee, S., Janssen, L., Calafat, J., Janssen, H., Wubbolts, R. & Neefjes, J. (2001) *Curr. Biol.* **11,** 1680–1685.
19. Burkhardt, J. K., Echeverri, C. J., Nilsson, T. & Vallee, R. B. (1997) *J. Cell Biol.* **139,** 469–484.
20. Harada, A., Takei, Y., Kanai, Y., Tanaka, Y., Nonaka, S. & Hirokawa, N. (1998) *J. Cell Biol.* **141,** 51–59.
21. Feng, L., Novak, E. K., Hartnell, L. M., Bonifacino, J. S., Collinson, L. M. & Swank, R. T. (2002) *Blood* **99,** 1651–1658.
22. Novak, E. K. & Swank, R. T. (1980) *Genet. Res.* **35,** 195–204.
23. Chiang, P.-W., Oiso, N., Gautam, R., Suzuki, T., Swank, R. T. & Spritz, R. A. (2003) *J. Biol. Chem.* **278,** 20332–20337.
24. Martina, J. A., Moriyama, K. & Bonifacino, J. S. (2003) *J. Biol. Chem.*, 10.1074/jbcM301294200.